Bioorg. Med. Chem. 29 (2021) 115876

Contents lists available at ScienceDirect

Bioorganic & Medicinal Chemistry

journal homepage: www.elsevier.com/locate/bmc

Discovery of 4-amino-1*H*-pyrazolo[3,4-*d*]pyrimidin derivatives as novel discoidin domain receptor 1 (DDR1) inhibitors

Ru Dong, Xin Zhou, Min Wang, Wen Li, Jin-Yang Zhang, Xin Zheng, Kai-Xiang Tang, Li-Ping Sun *

Jiangsu Key Laboratory of Drug Design & Optimization, Department of Medicinal Chemistry, China Pharmaceutical University, Nanjing 210009, PR China

ARTICLE INFO

Keywords:
DDR1 inhibitors
4-amino-1*H*-pyrazolo[3,4-*d*]pyrimidin
Cancer treatment
Molecular docking

ABSTRACT

DDR1 is a receptor tyrosine kinase that is activated by triple-helical collagens and has become an attractive target for anticancer therapy given its involvement in tumor growth, metastasis development, and tumor dormancy. Several drugs on the market, such as dasatinib and nilotinib, were reported to potently suppress the function of DDR1 and show significant therapeutic benefits in a variety of preclinical tumor models. Whereas only a few selective DDR1 inhibitors were disclosed in recent years. A series of 4-amino-1*H*-pyrazolo[3,4-*d*]pyrimidin derivatives were designed and synthesized. All compounds were evaluated via DDR1 kinase inhibition assay and cell anti-proliferative assay. One of the representative compounds, **6c**, suppressed DDR1 kinase activity with an IC_{50} value of 44 nM and potently inhibited cell proliferation in DDR1-overexpressing cell lines HCT-116 and MDA-MB-231 with IC_{50} value of 4.00 and 3.36 μM respectively. Further molecular docking study revealed that **6c** fitted ideally into DDR1 binding pocket and maintained the crucial hydrogen bonds with DDR1 kinase domain. Overall, these results suggest that the compound **6c** is a potential DDR1 inhibitor deserving further investigation for cancer treatment.

1. Introduction

Discoidin domain receptors (DDRs), classified into two types: DDR1 and DDR2, are receptor tyrosine kinases (RTKs)[1]. DDRs regulate basic aspects of cell behaviors (cellular morphogenesis, differentiation, proliferation, adhesion, migration, and invasion) by interacting with collagen and cross-talking with different types of cell surface receptors (such as integrins and other RTKs)[2]. Increasing studies have reported that DDRs play the part of potential oncogenic drivers in various cancers, including lung cancer, breast cancer, brain cancer, prostate cancer, leukemia, colorectal cancer, liver cancer, and so on[3]. Moreover, DDRs are linked closely with fibrotic disorders[4–6] and atherosclerosis[7–9]. A survey revealed that nilotinib strongly inhibited human colon cancer cells (CRC) invasion in vitro and reduced their metastatic potential in intrasplenic tumor mouse models and patient-derived metastatic and circulating CRC cell lines by inhibiting the kinase activity of DDR1[10]. Other surveys showed that inhibition of DDR1 sensitized glioblastoma cells to radio- and chemotherapy by inducing autophagy[11,12]. Silencing DDR1 by siRNA reduced metastatic activity in lung cancer models and enhanced the chemosensitivity of breast cancer cells to genotoxic drugs[13–15]. Therefore, DDR1 has been considered as a promising drug target for anticancer or other diseases' therapy.

Until recently, several small molecules[16–21] were reported to potently and selectively suppress the kinase activity of DDR1 (Fig. 1), with IC_{50} of low nanomole. In 2013, the compound **7rh** as a first selective DDR1 inhibitor was reported to effectively inhibit the proliferation, invasion, adhesion, and tumorigenicity of cancer cells with high DDR1 expression[16]. A research showed **7rh** strongly inhibited gastric cancer (GC) tumor growth, supporting the potential of DDR1-induced mechanisms for clinical GC therapy[22]. The compound **5** potently suppressed collagen-induced DDR1 signaling and epithelial-mesenchymal transition, and exhibited promising therapeutic efficacy in orthotopic mouse models of pancreatic cancer[21]. All those surveys show that DDR1 is becoming an attractive target for drug discovery.

There will still be a rise in the demand for DDR1 targeted therapies. A series of 4-amino-1*H*-pyrazolo[3,4-*d*]pyrimidin derivatives were designed and synthesized (Scheme 1). Based on high homology in the ATP-binding pocket, core scaffolds of tyrosine kinase inhibitors were screened to occupy the adenine portion of the DDR1 ATP-binding pocket using Discovery Studio 3.0, and new inhibitors were eventually designed

* Corresponding author.
E-mail address: chslp@cpu.edu.cn (L.-P. Sun).

https://doi.org/10.1016/j.bmc.2020.115876
Received 29 September 2020; Received in revised form 8 November 2020; Accepted 9 November 2020
Available online 17 November 2020

by combining the core scaffold screened and the fragment of DDR1-IN-1 (Fig. 2). Moreover, the potential efficacy of these compounds was evaluated in vitro.

2. Results and discussions

2.1. Chemistry

The general schemes for the synthesis of compounds **6a**~**6u** were summarized in Scheme 1. The key steps were copper-catalyzed Ullmann coupling reaction[23] and palladium-catalyzed Suzuki coupling reaction[24]. Briefly, commercially available 2-iodo-4-nitro-toluene (**7**) was treated with phenol (**8**) under copper catalysis to afford the Ullmann coupling product (**9**), which went through iodization to yield the compound (**10**). Then, the intermediate (**10**) was reacted with bis(pinacolato)diboron under palladium catalysis to produce the compound (**11**), which was hydrolyzed to obtain the product (**12**). The compound (**12**) went through palladium-catalyzed Suzuki coupling reaction with commercially available compound (**13**) to afford the intermediate (**14**), which was reduced to the aromatic amine (**15**). In the end, the intermediate (**15**) and the synthesized acyl chloride (**16**) went through amide condensation to afford the target compounds (**6a**~**6u**).

2.2. In vitro kinase inhibitory activities

To explore the inhibitory activities of the designed compounds, these compounds were evaluated using the LANCE ULTRA kinase assay. The results are summarized in Table 1. **GZD856** was used as a positive control for its strong binding affinity to DDR1[25]. Compounds **6c**, **6d**, and **6u** inhibited DDR1 with IC_{50} values ranging from 0.044 to 0.070 μM. Accordingly, substituents of hydrogen (**6u**) or methyl (**6c**) group at R_1 could be tolerated without reducing the inhibitory activity against DDR1. Whereas it seemed that substituents on the *N*-terminal phenyl ringdrama-tically impacted DDR1 kinase inhibition. When (4-methylpiperazin-1-yl)methylene substituent (**6c**, IC_{50} = 44 nM) was replaced by (4-ethylpiperazin-1-yl)methylene substituent (**6d**, IC_{50} = 70 nM) at R_3, the DDR1 inhibitory activity was reduced. When (4-methylpiperazin-1-yl)methylene group was introduced at R_2, the resulting compound (**6e**) showed twice as potent as the compound (**6a**) containing (4-methylpiperazin-1-yl)methylene group at R_3. However, the potency of compounds (**6j**, **6k**, **6l**, and **6m**) which contained other alicyclic amines at R_3 was significantly decreased. When iodo group was introduced at R_2, the IC_{50} value of the compound (**6i**) was 131.0 nM, less potent than **6c**. Besides, the compounds (**6p**, **6r**, and **6t**) with halo substituents at R_2 displayed significantly weaker DDR1 inhibitory activities than the compound (**6k**) with trifluoromethyl substituent. As a result, the compound with trifluoromethyl substituent at R_2 and (4-methylpiperazin-1-yl)methylene group at R_3 showed the most potent DDR1 inhibitory activity.

2.3. Inhibition of cell proliferation

To determine their inhibitory activities of cell proliferation, all designed compounds were evaluated against two cancer cell lines expressing high level of DDR1 by MTT assay. The results are shown in Table 2, and **nilotinib** was selected as the positive control because of its strong DDR1 inhibitory activity. As shown in Table 2, all of the compounds were evaluated their inhibition of DDR1-overexpressing cancer cell lines and most of them exhibited significantly anti-proliferative activities (>95%) at the concentration of 10 μM. Then the compounds, inhibiting >95% cell proliferation, were tested their IC_{50} values. It was surprising that most of the compounds showed better anti-proliferative activities than **nilotinib**. Especially, compound **6c** potently inhibited cell proliferation in cell lines HCT-116 and MDA-MB-231 with IC_{50} values of 4.00 and 3.36 μM respectively. The results indicated that **6c** could be a promising lead compound for cancer treatment.

2.4. Molecular docking study

To further elucidate the interaction between the compound **6c** and DDR1, Discovery Studio 4.0/CDOCKER protocol was employed to analyze the possible binding mode. The binding mode of the most potent compound **6c** and DDR1 is shown in Fig. 3. The results suggested that the compound **6c** could bind tightly with the DDR1 kinase via four hydrogen bonds, two π-π stacked interactions, electrostatic interactions, and many Van der Waals interactions. As expected, the nitrogen atom and the secondary amino hydrogen atom at the 1*H*-pyrazolo[3,4-*d*]pyrimidin moiety formed two essential hydrogen bonds with the secondary amino hydrogen atom (2.4 Å, 173.1°) and the carbonyl oxygen atom (2.3 Å, 134.7°) of Met^{704} in the hinge binding area respectively, which might play a deciding role in the binding affinity with DDR1 kinase. Besides, 1*H*-pyrazolo[3,4-*d*]pyrimidin generated π-π interactions with the phenyl ring of the residue Tyr^{703} (Figure C), indicating that the 1*H*-pyrazolo[3,4-*d*]pyrimidin moiety plays an important role in the combination of the receptor and the ligand. Moreover, Glu^{672} in the αC-helix and Asp^{784} in the DFG motif formed two hydrogen bonds with the linker amide moiety, the distances of which were 2.3 Å (127.5°) and 2.1 Å (170.4°) respectively, contributing to the affinity increment of compound **6c** with DDR1. These results revealed that the compound **6c** had a good binding ability to DDR1 kinase as designed and explained the high potency of inhibition on DDR1 Kinase.

3. Conclusion

In summary, a new class of 4-amino-1*H*-pyrazolo[3,4-*d*]pyrimidin compounds have been designed and synthesized, and their DDR1 inhibitory activities and anti-proliferative activities were evaluated in vitro. It was found that compound **6c** exhibited robust potency of DDR1 inhibition with an IC_{50} value of 44 nM. Besides, compound **6c** potently

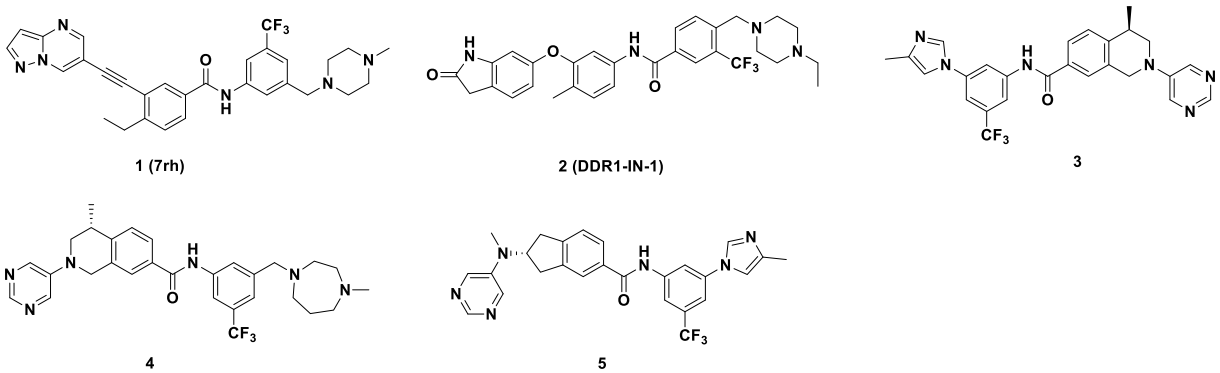

Fig. 1. Part of reported selective DDR1 inhibitors.

inhibited proliferation of cancer cell lines expressing high levels of DDR1 with IC_{50} values in low micromole range. These findings demonstrate that the compound **6c** can be a potent DDR1 inhibitor and worthy of further investigation.

4. Experiment

4.1. Chemistry

All reagents and solvents were purchased from commercial sources without further purification. Flash chromatography was performed using 300-mesh silica gel. All reactions were monitored by TLC using silica gel plates with fluorescence F254 and UV-light visualization. ^{1}H NMR spectra and ^{13}C NMR spectra were recorded on a Bruker AV-300 spectrometer at 300 MHz. Coupling constants (J) are expressed in hertz (Hz). Chemical shifts (δ) of NMR are reported in parts per million (ppm) relative to an internal standard (TMS). ESI-MS spectra were recorded on an Agilent/HP 1100 Series LC/MSD Trap SL mass spectrometer. High resolution mass spectrometry (HRMS) was obtained on a Q-tof high resolution mass spectrometer. Melting points (uncorrected) were determined on a RY-1 MP apparatus. The IR spectra was recorded on a Nicolet Impact 410 infrared spectrometer.

4.2. General procedure for the preparation of the compounds (6a~6u)

*1-methyl-4-nitro-2-phenoxybenzene (**9**).* A mixture of 2-iodo-4-nitrotoluene (**7**) (1052.1 mg, 4 mmol), phenol (**8**) (564.7 mg, 6 mmol), Cs_2CO_3 (2606.6 mg, 8 mmol), CuI (152.4 mg, 0.8 mmol), and *N, N*-dimethylglycine hydrochloride (355.0 mg, 2.4 mmol), and anhydrous 1,4-dioxane (15 mL) in a schlink tube was heated at 135 °C under nitrogen atmosphere. After the reaction completed monitored by TLC, the cooled mixture was partitioned between ethyl acetate and water. The organic layer was separated, and the aqueous layer was extracted with ethyl acetate. The combined organic layers were washed with brine, dried over anhydrous Na_2SO_4, and concentrated in vacuo. The residual oil was loaded on a silica gel column and eluted with ethyl acetate/petroleum ether (1/100) to afford the product (778.9 mg, 85.0%). ^{1}H NMR (300 MHz, Chloroform-d) δ 7.95 (dd, *J* = 8.3, 2.3 Hz, 1H), 7.70 (d, *J* = 2.3 Hz, 1H), 7.48–7.40 (m, 3H), 7.23 (tt, *J* = 7.2, 1.0 Hz, 1H), 7.07–7.01 (m, 2H), 2.45 (s, 3H).

*2-(4-iodophenoxy)-1-methyl-4-nitrobenzene (**10**).* To a 100 mL round-bottomed flask wereadded 1-methyl-4-nitro-2-phenoxybenzene (1507.9 mg, 6.58 mmol), *N*-iodosuccinimide (1481.0 g, 6.71 mmol), $FeCl_3$ (107.1 mg, 0.66 mmol), and acetonitrile (20 mL), and the mixture was stirred at 60 °C. After the reaction completed monitored by TLC, ethyl acetate was added, and the organic phase was washed with brine (3 times), which was dried over anhydrous Na_2SO_4. The residual oil was loaded on a silica gel column and eluted with ethyl acetate/petroleum ether (1/100) to afford the product (1844.4 mg, 80.0%). ^{1}H NMR (300 MHz, Chloroform-*d*) δ 7.94 (dd, *J* = 8.3, 2.0 Hz, 1H), 7.74–7.63 (m, 3H), 7.42 (d, *J* = 8.3 Hz, 1H), 6.77 (d, *J* = 8.8 Hz, 2H), 2.39 (s, 3H).

*4,4,5,5-tetramethyl-2-(4-(2-methyl-5-nitrophenoxy)phenyl)-1,3,2-dioxaborolane (**11**).* To asolution of 2-(4-iodophenoxy)-1-methyl-4-nitrobenzene (1844.4 mg, 5.20 mmol) in anhydrous 1,4-dioxane (20 mL) were added 1,1′-bis(diphenylphosphino)ferrocene dichloropalla-dium (II) (380.5 mg, 0.1 mmol), bis(pinacolato)diboron (1979.2 mg, 1.5 mmol), and potassium acetate (1531.0 mg, 15.6 mmol). The reaction mixture was stirred at 101 °C. After the reaction completed monitored by TLC, the cooled mixture was filtered. The filtrate was concentrated in vacuo, resuspended in ethyl acetate and water, and separated. The organic layer was extracted with brine and dried over anhydrous Na_2SO_4. Purification by silica gel chromatography with ethyl acetate/petroleum ether (1/20) provided the product as white solid(1613.0 mg, 87.3%). ^{1}H NMR (300 MHz, Chloroform-*d*) δ 7.92 (dd, *J* = 8.4, 2.3 Hz, 1H), 7.86–7.79 (m, 2H), 7.69 (d, *J* = 2.3 Hz, 1H), 7.40 (d, *J* = 8.4 Hz, 1H), 6.99–6.92 (m, 2H), 2.36 (s, 3H), 1.35 (s, 12H).

*(4-(2-methyl-5-nitrophenoxy)phenyl)boronic acid (**12**).* 4,4,5,5-tetramethyl-2-(4-(2-methyl-5-nitrophenoxy)phenyl)-1,3,2-dioxaborolane (441.4 mg, 1.24 mmol) and sodium periodate (795.7 mg, 3.72 mmol) were stirred in 5 mL of a 4:1 mixture of THF and water for 30 min, at

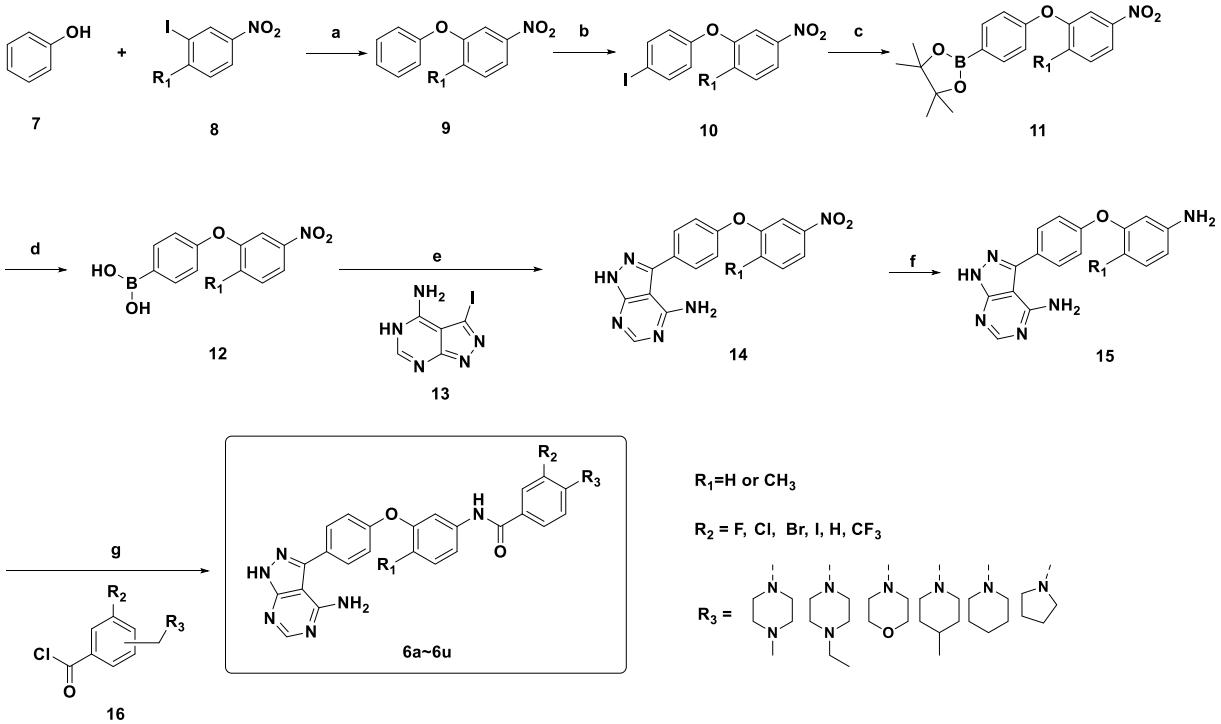

Scheme 1. Synthesis of 4-amino-1*H*-pyrazolo[3,4-*d*]pyrimidin derivatives. Reagents and conditions: (a) Cs_2CO_3, CuI, *N*,*N*-dimethylglycine hydrochloride, Dioxane, 135 °C; (b) NIS, $FeCl_3$, CH_3CN, 60 °C; (c) $Pd(dppf)Cl_2$, KOAc, Dioxane, 100 °C; (d) $NaIO_4$, 1 M HCl, THF: H_2O (4: 1), 25 °C; (e) $Pd(dppf)Cl_2$, $K_3PO_4 \cdot 3H_2O$, THF/H_2O = 4/1, 100 °C; (f) activated carbon, $FeCl_3$, 80% Hydrazine Hydrate, EtOH, 85 °C; (g) TEA, absolute THF, 65 °C

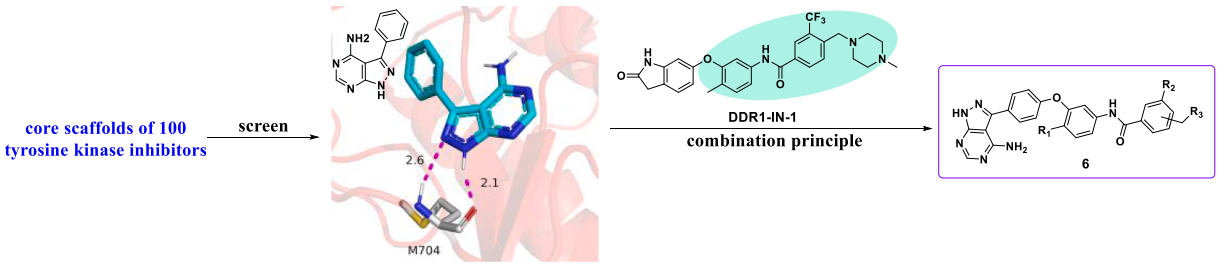

Fig. 2. Design of 4-amino-1*H*-pyrazolo[3,4-*d*]pyrimidin derivatives as novel DDR1 inhibitors.

Table 1

In vitro kinase inhibitory activities of compounds 6a~6u against DDR1.

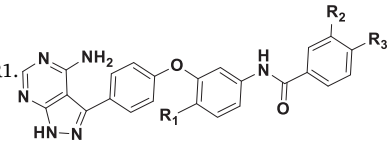

Cpds	R_1	R_2	R_3	IC_{50} (μM)	Cpds	R_1	R_2	R_3	IC_{50} (μM)
6a	CH_3	H	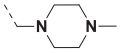	2.694	**6l**	CH_3	CF_3		0.975
6b	CH_3	H		N.D.	**6m**	CH_3	CF_3	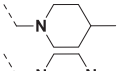	2.810
6c	CH_3	CF_3	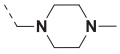	0.044	**6n**	CH_3	H		N.D.
6d	CH_3	CF_3	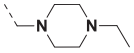	0.070	**6o**	CH_3	F	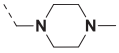	N.D.
6e	CH_3		H	1.213	**6p**	CH_3	F	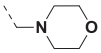	24.350
6f	CH_3	H	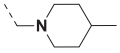	N.D.	**6q**	CH_3	Cl	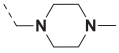	N.D.
6g	CH_3	H		N.D.	**6r**	CH_3	Cl	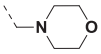	2.172
6h	CH_3	H	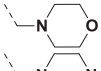	N.D.	**6s**	CH_3	Br	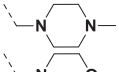	N.D.
6i	CH_3	I	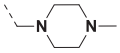	0.131	**6t**	CH_3	Br	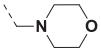	2.468
6j	CH_3	CF_3		1.189	**6u**	H	CF_3	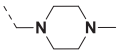	0.044
6k	CH_3	CF_3	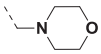	0.416	**GZD856**				0.005

DDR1 experiments were performed using the LANCE ULTRA kinase assay, according to the manufacturer's instructions. The data is from one experiment. N.D. = Not determined.

which time aqueous hydrochloric acid (1 N, 0.87 mL, 0.87 mmol) was added to the suspension. The reaction mixture was stirred at ambient temperature. After TLC showed complete consumption of the arylboronic acid ester, the reaction mixture was diluted with water and extracted with ethyl acetate. The combined extracts were washed with water and brine, dried over sodium sulfate, filtered, and concentrated to dryness by rotary evaporation. The residue was purified by silica gel chromatography with ethyl acetate/petroleum ether (1/2), giving the product as white solid(185.6 mg, 54.8%).

*3-(4-(2-methyl-5-nitrophenoxy)phenyl)-1H-pyrazolo[3,4-d]pyrimidin-4-amine (**14**).* To amixture of 3-iodo-5*H*-pyrazolo[3,4-*d*]pyrimidin-4-amine (871.6 mg, 3.34 mmol) and THF/H_2O (40 mL, v/v, 4/1) were added (4-(2-methyl-5-nitrophenoxy)phenyl)boronic acid (1184.4 mg, 4.34 mmol), $K_3PO_4{\cdot}3H_2O$ (2663.1 mg, 10.0 mmol), and Pd(dppf)Cl_2 (490.2 mg, 0.67 mmol). The reaction mixture was placed into an oil bath preheated to 100 °C, with stirring at this temperature under nitrogen. After the reaction completed monitored by TLC, the resulting mixture was filtered through a celite pad and concentrated to dryness by rotary evaporation. The residue was purified by silica gel chromatography with DCM/MeOH (80/1, 1% TEA) to afford the product as a white color solid (622.3 mg, 51.42%). ^{1}H NMR (300 MHz, DMSO-d_6) δ 13.64 (s, 1H), 8.26 (s, 1H), 8.05 (dd, J = 8.4, 2.3 Hz, 1H), 7.87–7.66 (m, 4H), 7.36–7.14 (m, 3H), 2.43 (s, 3H).

*3-(4-(5-amino-2-methylphenoxy)phenyl)-1H-pyrazolo[3,4-d]pyrimidin-4-amine (**15**).* The solu- tion of 3-(4-(2-methyl-5-nitrophenoxy) phenyl)-1*H*-pyrazolo[3,4-*d*]pyrimidin-4-amine (622.3 mg, 1.72 mol) and ethanol (26.8 mL) was stirred at 60 °C, an appropriate amount of activated carbon (60.2 mg) and ferric chloride (62.0 mg) were added at the temperature, the mixture was heated to 85 °C and 80 percent hydrazine hydrate (5.7 mL) was added to the solution. The reaction mixture then was refluxed for 2 h and monitored by TLC. The mixture was filtered and the precipitate was washed with ethanol. The filtrate was concentrated under reduced pressure and the residue was poured into water with stirring for 30 min. The precipitate was filtered and dried to furnish the product as white solid (480.3 mg, 84.0%). ^{1}H NMR (300 MHz, DMSO-d_6) δ 13.54 (s, 1H), 8.23 (s, 1H), 7.64 (d, J = 6.9 Hz, 2H), 7.13–6.90 (m, 3H), 6.39 (d, J = 6.1 Hz, 1H), 6.25 (s, 1H), 5.05 (s, 2H), 2.03 (s, 3H).

N-(3-(4-(4-amino-1H-pyrazolo[3,4-d]pyrimidin-3-yl)phenoxy)-4-methylphenyl)-4-((4-methyl-piperazin-1-yl)methyl)benzamide (**6a**). A 25 mL round bottom flask charged with 3-(4-(5-amino-2- methylphenoxy) phenyl)-1*H*-pyrazolo-[3,4-*d*]pyrimidin-4-amine(7) (50.0 mg, 0.18 mmol), THF (5 mL), Et_3N (0.05 mL, 0.36 mmol) treated with 4-((4-methylpiperazin-1-yl)methyl)benzoyl chloride (8) (about 0.25 mmol).

Table 2
The anti-proliferative effects of compounds on two cancer cells harboring high levels of DDR1.

Cpds	HCT-116		MDA-MB-231	
	Inhibition at 10 μM (%)	IC_{50} (μM)	Inhibition at 10 μM (%)	IC_{50} (μM)
6a	26.70 ± 8.01	>10	94.54 ± 0.57	N.D.
6b	99.59 ± 0.21	2.00 ± 0.19	98.70 ± 0.37	2.68 ± 0.26
6c	99.96 ± 0.04	4.00 ± 0.12	97.93 ± 1.15	3.36 ± 0.11
6d	99.74 ± 0.09	5.48 ± 0.21	99.28 ± 0.77	3.85 ± 0.07
6e	99.83 ± 0.04	4.47 ± 0.28	99.28 ± 0.38	N.D.
6f	99.94 ± 0.30	1.37 ± 0.03	97.40 ± 0.37	2.76 ± 0.02
6	99.96 ± 0.11	3.04 ± 0.04	98.83 ± 0.55	N.D.
6h	97.25 ± 0.89	4.89 ± 0.08	98.96 ± 0.74	3.53 ± 0.08
6i	99.74 ± 0.09	4.51 ± 0.02	98.87 ± 0.19	3.21 ± 0.07
6j	34.86 ± 0.76	>10	98.47 ± 0.00	N.D.
6k	20.50 ± 1.74	>10	71.28 ± 2.87	N.D.
6l	36.91 ± 8.32	>10	29.62 ± 0.96	>10
6m	73.73 ± 1.16	N.D.	42.06 ± 2.10	>10
6n	33.63 ± 1.00	>10	88.67 ± 1.29	N.D.
6o	73.25 ± 3.68	N.D.	92.06 ± 0.18	N.D.
6p	11.09 ± 7.21	>10	93.06 ± 0.00	N.D.
6q	99.91 ± 0.15	2.91 ± 0.12	99.22 ± 0.37	3.83 ± 0.39
6r	58.26 ± 6.05	N.D.	96.48 ± 0.92	N.D.
6s	99.55 ± 0.05	6.56 ± 0.80	100.00 ± 0.37	N.D.
6t	35.02 ± 9.04	>10	81.29 ± 2.87	N.D.
6u	99.85 ± 0.16	5.96 ± 0.06	98.20 ± 0.38	4.29 ± 0.01
Nilotinib	88.14 ± 0.02	5.75 ± 0.10	93.60 ± 0.77	7.31 ± 0.17

Biological activity data on inhibition of cancer cell lines were expressed as the means ± SD derived from three independent measurements. N.D. = not determined.

The reaction mixture was stirred at room temperature. After the reaction completed monitored by TLC, then Saturated sodium bicarbonate solution was added. The reaction mixture was extracted with ethyl acetate. The organic layers were combined and washed with brine, and then dried over anhydrous Na_2SO_4. The resulting residue was purified by TLC on a silica gel (DCM: MeOH = 40: 1, 2% TEA), then was beaten in CH_3CN at 80 °C for 12 h. The mixture was cooled to room temperature and filtered to afford the product as white solid(17.5 mg, 21.26%). Mp: 179~180 °C. ^{1}H NMR (300 MHz, DMSO-d_6) δ 13.56 (s, 1H), 10.24 (s, 1H), 8.21 (s, 1H), 7.87 (d, J = 7.9 Hz, 2H), 7.66 (d, J = 8.2 Hz, 2H), 7.57 (dd, J = 5.3, 1.7 Hz, 2H), 7.42 (d, J = 7.9 Hz, 2H), 7.32 (d, J = 8.7 Hz, 1H), 7.08 (d, J = 8.4 Hz, 2H), 6.79 (s, 1H), 3.51 (d, J = 4.8 Hz, 2H), 2.36 (s, 7H), 2.18 (d, J = 8.5 Hz, 6H). HRMS (ESI+) m/z calculated for $\mathbf{C_{31}H_{32}N_8O_2}$ [M+H]$^+$, 549.2721; found,549.2723.

N-(3-(4-(4-amino-1H-pyrazolo[3,4-d]pyrimidin-3-yl)phenoxy)-4-methylphenyl)-4-(piperidin-1-yl-methyl)benzamide ***(6b)***. Prepared in the same manner as **6a**. Yield: 26.8%, mp: 204~205 °C. ^{1}H NMR (300 MHz, DMSO-d_6) δ 13.56 (s, 1H), 10.24 (s, 1H), 8.21 (s, 1H), 7.86 (d, J = 7.8 Hz, 2H), 7.66 (d, J = 8.5 Hz, 2H), 7.57 (d, J = 6.1 Hz, 2H), 7.41 (d, J = 7.8 Hz, 2H), 7.32 (d, J = 8.6 Hz, 1H), 7.08 (d, J = 8.6 Hz, 2H), 3.49 (s, 2H), 2.32 (s, 4H), 2.19 (s, 3H), 1.49 (s, 4H), 1.38 (s, 2H). HRMS (ESI+) m/z calculated for $\mathbf{C_{31}H_{31}N_7O_2}$ [M+H]$^+$, 534.2612; found,534.2620.

N-(3-(4-(4-amino-1H-pyrazolo[3,4-d]pyrimidin-3-yl)phenoxy)-4-methylphenyl)-4-((4-methyl-piperazin-1-yl)methyl)-3-(trifluoromethyl)benzamide ***(6c)***. Prepared in the same manner as **6a**. Yield: 23.2%, mp: 160~161 °C. ^{1}H NMR (300 MHz, DMSO-d_6) δ 13.56 (s, 1H), 10.46 (s, 1H), 8.25–8.13 (m, 3H), 7.90 (d, J = 8.0 Hz, 1H), 7.72–7.62 (m, 2H), 7.62–7.50 (m, 2H), 7.34 (d, J = 8.2 Hz, 1H), 7.16–7.04 (m, 2H), 6.81 (s, 1H), 3.67 (s, 2H), 2.40 (s, 8H), 2.19 (d, J = 7.2 Hz, 6H). HRMS (ESI+) m/z calculated for $\mathbf{C_{32}H_{31}F_3N_8O_2}$ [M+H]$^+$, 617.2595; found, 617.2590.

N-(3-(4-(4-amino-1H-pyrazolo[3,4-d]pyrimidin-3-yl)phenoxy)-4-methylphenyl)-4-((4-ethyl-piperazin-1-yl)methyl)-3-(trifluoromethyl)benzamide ***(6d)***. Prepared in the same manner as **6a**. Yield: 22.8%, mp: 158~160 °C. ^{1}H NMR (300 MHz, DMSO-d_6) δ 13.54 (s, 1H), 10.44 (s, 1H), 8.28–8.09 (m, 3H), 7.88 (d, J = 8.0 Hz, 1H), 7.65 (d, J = 8.3 Hz, 2H), 7.60–7.46 (m, 2H), 7.32 (d, J = 8.2 Hz, 1H), 7.07 (d, J = 8.2 Hz, 2H), 6.78 (s, 1H), 3.64 (s, 2H), 2.45–2.26 (m, 8H), 2.18 (s, 3H), 0.96 (t, J = 7.0 Hz, 3H). HRMS (ESI+) m/z calculated for $\mathbf{C_{33}H_{33}F_3N_8O_2}$ [M+H]$^+$, 631.2751; found,631.2752.

N-(3-(4-(4-amino-1H-pyrazolo[3,4-d]pyrimidin-3-yl)phenoxy)-4-methylphenyl)-3-((4-methyl-piperazin-1-yl)methyl)benzamide ***(6e)***. Prepared in the same manner as **6a**. Yield: 42.0%, mp: 166~168 °C. ^{1}H NMR (300 MHz, DMSO-d_6) δ 13.55 (s, 1H), 10.26 (s, 1H), 8.22 (s, 1H), 7.81 (d, J = 6.8 Hz, 2H), 7.67 (d, J = 8.2 Hz, 2H), 7.58 (d, J = 6.5 Hz, 2H), 7.46 (d, J = 8.6 Hz, 2H), 7.33 (d, J = 8.5 Hz, 1H), 7.09 (d, J = 8.2 Hz, 2H), 6.81 (s, 1H), 3.51 (s, 2H), 2.36 (s, 7H), 2.20 (s, 3H), 2.14 (s, 3H). HRMS (ESI+) m/z calculated for $\mathbf{C_{31}H_{32}N_8O_2}$ [M+H]$^+$, 549.2721; found,549.2728.

N-(3-(4-(4-amino-1H-pyrazolo[3,4-d]pyrimidin-3-yl)phenoxy)-4-methylphenyl)-4-((4-methyl-piperidin-1-yl)methyl)benzamide ***(6f)***. Prepared in the same manner as **6a**. Yield: 13.2%, mp: 198~199 °C. ^{1}H NMR (300 MHz, DMSO-d_6) δ 13.58 (s, 1H), 10.26 (s, 1H), 8.24 (s, 1H), 7.89 (d, J = 8.2 Hz, 2H), 7.74–7.65 (m, 2H), 7.61 (dq, J = 4.7, 2.1 Hz, 2H), 7.44 (d, J = 8.0 Hz, 2H), 7.35 (d, J = 8.9 Hz, 1H), 7.16–7.08 (m, 2H), 6.82 (s, 1H), 3.52 (s, 2H), 2.78 (d, J = 11.1 Hz, 2H), 2.22 (s, 3H), 1.95 (t, J = 11.2 Hz, 2H), 1.58 (dd, J = 12.2, 3.3 Hz, 2H), 1.32 (s, 1H), 1.18 (td, J = 12.0, 3.7 Hz, 2H), 0.91 (d, J = 6.3 Hz, 3H). HRMS (ESI+) m/z calculated for $\mathbf{C_{32}H_{33}N_7O_2}$ [M+H]$^+$, 548.2768; found,548.2779.

N-(3-(4-(4-amino-1H-pyrazolo[3,4-d]pyrimidin-3-yl)phenoxy)-4-methylphenyl)-4-(pyrrolidin-1-yl-methyl)benzamide ***(6g)***. Prepared in the same manner as **6a**. Yield: 43.5%, mp: 166~167 °C. ^{1}H NMR (300 MHz, DMSO-d_6) δ 13.58 (s, 1H), 10.25 (s, 1H), 8.24 (s, 1H), 7.90 (d, J = 7.8 Hz, 2H), 7.69 (d, J = 8.2 Hz, 2H), 7.61 (s, 2H), 7.45 (d, J = 7.8 Hz, 2H), 7.34 (d, J = 8.5 Hz, 1H), 7.11 (d, J = 8.1 Hz, 2H), 6.78 (s, 1H), 3.66 (s, 2H), 2.46 (s, 4H), 2.22 (s, 3H), 1.72 (s, 4H). HRMS (ESI+) m/z calculated for $\mathbf{C_{30}H_{29}N_7O_2}$ [M+H]$^+$, 520.2455; found, 520.2460.

N-(3-(4-(4-amino-1H-pyrazolo[3,4-d]pyrimidin-3-yl)phenoxy)-4-methylphenyl)-4-(morpholino-methyl)benzamide ***(6h)***. Prepared in the same manner as **6a**. Yield: 7.7%, mp: 182~184 °C. ^{1}H NMR (300 MHz, DMSO-d_6) δ 13.59 (s, 1H), 10.30 (s, 1H), 8.25 (s, 1H), 7.94 (d, J = 7.7 Hz, 2H), 7.70 (d, J = 8.3 Hz, 2H), 7.61 (s, 2H), 7.52 (s, 2H), 7.36 (d, J = 8.8 Hz, 1H), 7.12 (d, J = 8.3 Hz, 2H), 3.64 (s, 6H), 2.44 (s, 3H), 2.23 (s, 3H). HRMS (ESI+) m/z calculated for $\mathbf{C_{30}H_{29}N_7O_3}$ [M+H]$^+$, 536.2405; found, 536.2411.

N-(3-(4-(4-amino-1H-pyrazolo[3,4-d]pyrimidin-3-yl)phenoxy)-4-methylphenyl)-3-iodo-4-((4-methylpiperazin-1-yl)methyl)benzamide ***(6i)***. Prepared in the same manner as **6a**. Yield: 49.9%, mp: 166~167 °C. ^{1}H NMR (300 MHz, DMSO-d_6) δ 13.57 (s, 1H), 10.33 (s, 1H), 8.37 (s, 1H), 8.22 (s, 1H), 7.91 (d, J = 8.0 Hz, 1H), 7.67 (d, J = 8.2 Hz, 2H), 7.57 (d, J = 8.9 Hz, 2H), 7.50 (d, J = 7.8 Hz, 1H), 7.33 (d, J = 8.2 Hz, 1H), 7.09 (d, J = 8.3 Hz, 2H), 3.50 (s, 2H), 2.44 (s, 4H), 2.35 (s, 4H), 2.18 (d, J = 9.4 Hz, 6H). HRMS (ESI+) m/z calculated for $\mathbf{C_{31}H_{31}IN_8O_2}$ [M+H]$^+$, 675.1687; found, 675.1689.

N-(3-(4-(4-amino-1H-pyrazolo[3,4-d]pyrimidin-3-yl)phenoxy)-4-methylphenyl)-4-(pyrrolidin-1-yl-methyl)-3-(trifluoromethyl)benzamide ***(6j)***. Prepared in the same manner as **6a**. Yield: 34.9%, mp: 148~149 °C. ^{1}H NMR (300 MHz, DMSO-d_6) δ 13.58 (s, 1H), 10.49 (s, 1H), 8.24 (s, 2H), 8.20 (s, 1H), 7.94 (d, J = 8.0 Hz, 1H), 7.70 (d, J = 8.2 Hz, 2H), 7.61 (d, J = 9.1 Hz, 1H), 7.58 (s, 1H), 7.37 (d, J = 8.2 Hz, 1H), 7.12 (d, J = 8.2 Hz, 2H), 6.76 (s, 1H), 3.83 (s, 2H), 2.24 (s, 3H), 1.76 (s, 4H). HRMS (ESI+) m/z calculated for $\mathbf{C_{31}H_{28}F_3N_7O_2}$ [M+H]$^+$, 588.2329; found, 588.2334.

N-(3-(4-(4-amino-1H-pyrazolo[3,4-d]pyrimidin-3-yl)phenoxy)-4-methylphenyl)-4-(morpholino- methyl)-3-(trifluoromethyl)benzamide ***(6k)***. Prepared in the same manner as **6a**. Yield: 37.9%, mp: 150~151 °C. ^{1}H

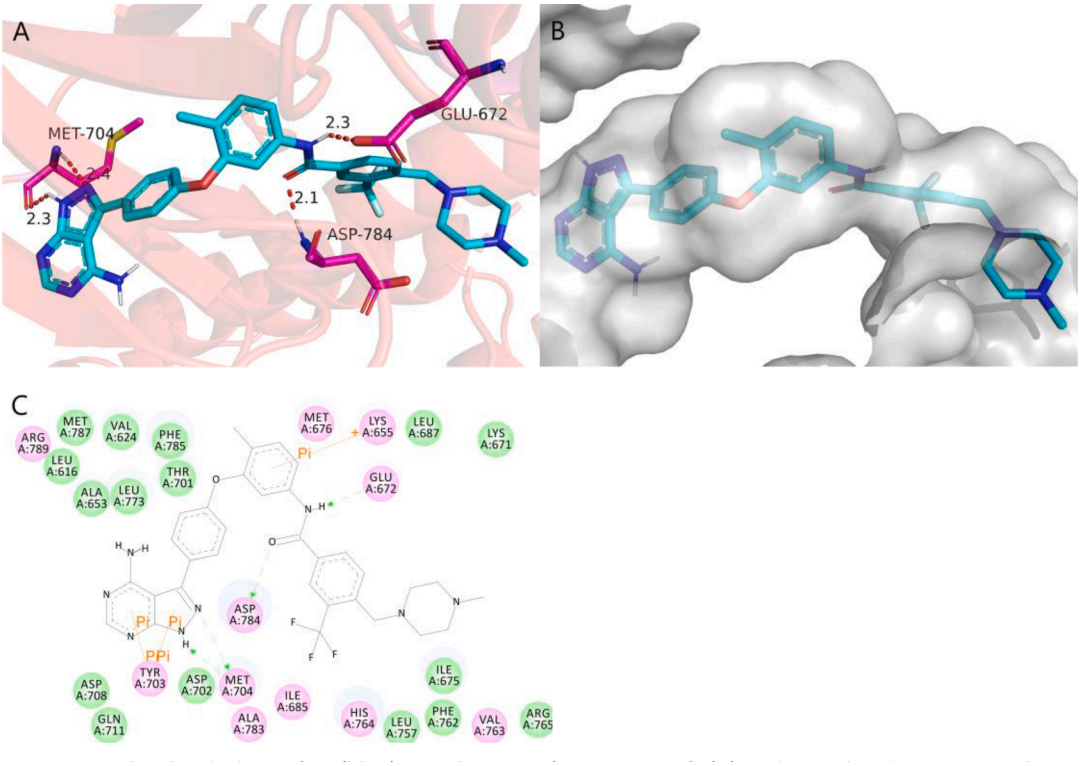

Fig. 3. Molecular docking of **6c** (blue) into the DDR1 (PDB ID: 4CKR). (A) Hydrogen-bond interactions between **6c** (in blue) and Met[704], Glu[672], and Asp[784], indicated by dash lines (B) Compound **6c** was fitted into the cavity of DDR1 kinase. (C) Compound **6c** interacted with residues in the DDR1 kinase domain. Residues in pink represented the electrostatic interactions with **6c,** and residues in green represented the Van der Waals interactions with **6c**.

NMR (300 MHz, DMSO-d_6) δ 13.56 (s, 1H), 10.47 (s, 1H), 8.21 (s, 3H), 7.93 (d, J = 8.4 Hz, 1H), 7.67 (d, J = 8.3 Hz, 2H), 7.57 (d, J = 9.9 Hz, 2H), 7.35 (d, J = 8.3 Hz, 1H), 7.09 (d, J = 8.4 Hz, 2H), 3.68 (s, 2H), 3.60 (s, 4H), 2.40 (s, 4H), 2.20 (s, 3H). HRMS (ESI+) m/z calculated for $\mathbf{C_{31}H_{28}F_3N_7O_3}$ [M+H]$^+$, 604.2278; found, 604.2282.

N-(3-(4-(4-amino-1H-pyrazolo[3,4-d]pyrimidin-3-yl)phenoxy)-4-methylphenyl)-4-(piperidin-1-yl-methyl)-3-(trifluoromethyl)benzamide ***(6l)***. Prepared in the same manner as **6a**. Yield: 35.6%, mp: 216~217 °C. ^{1}H NMR (300 MHz, DMSO-d_6) δ 13.59 (s, 1H), 10.50 (s, 1H), 8.28–8.17 (m, 3H), 7.96 (d, J = 8.2 Hz, 1H), 7.75–7.67 (m, 2H), 7.66–7.57 (m, 2H), 7.38 (d, J = 8.2 Hz, 1H), 7.17–7.09 (m, 2H), 6.78 (s, 1H), 3.66 (s, 2H), 2.39 (s, 4H), 2.24 (s, 3H), 1.63–1.38 (m, 6H). HRMS (ESI+) m/z calculated for $\mathbf{C_{32}H_{30}F_3N_7O_2}$ [M+H]$^+$, 602.2486; found, 602.2489.

N-(3-(4-(4-amino-1H-pyrazolo[3,4-d]pyrimidin-3-yl)phenoxy)-4-methylphenyl)-4-((4-methyl-piperidin-1-yl)methyl)-3-(trifluoromethyl)benzamide ***(6m)***. Prepared in the same manner as **6a**. Yield: 40.5%, mp: 242~243 °C. ^{1}H NMR (300 MHz, DMSO-d_6) δ 13.55 (s, 1H), 10.45 (s, 1H), 8.19 (t, 3H), 7.91 (d, J = 8.0 Hz, 1H), 7.67 (d, J = 8.2 Hz, 2H), 7.57 (d, J = 11.6 Hz, 2H), 7.34 (d, J = 8.2 Hz, 1H), 7.09 (d, J = 7.9 Hz, 2H), 3.63 (s, 2H), 2.73 (d, J = 10.0 Hz, 2H), 2.20 (s, 3H), 1.99 (t, J = 10.9 Hz, 2H), 1.57 (d, J = 12.5 Hz, 2H), 1.26–1.05 (m, 2H), 0.89 (d, J = 6.5 Hz, 3H).HRMS (ESI+) m/z calculated for $\mathbf{C_{33}H_{32}F_3N_7O_2}$ [M+H]$^+$, 616.2642; found, 616.2647.

N-(3-(4-(4-amino-1H-pyrazolo[3,4-d]pyrimidin-3-yl)phenoxy)-4-methylphenyl)-4-((4-ethyl-piperazin-1-yl)methyl)benzamide ***(6n)***. Prepared in the same manner as **6a**. Yield: 18.6%, mp: 276~277 °C. ^{1}H NMR (300 MHz, DMSO-d_6) δ 13.55 (s, 1H), 10.23 (s, 1H), 8.21 (s, 1H), 7.87 (d, J = 8.0 Hz, 2H), 7.69–7.64 (m, 2H), 7.60–7.55 (m, 2H), 7.42 (d, J = 8.0 Hz, 2H), 7.32 (d, J = 8.8 Hz, 1H), 7.11–7.06 (m, 2H), 3.51 (s, 2H), 2.46–2.23 (m, 10*H*), 2.19 (s, 3H), 0.97 (t, J = 7.2 Hz, 3H). HRMS (ESI+ESI+) m/z calculated for $\mathbf{C_{32}H_{34}N_8O_2}$ [M+H]$^+$, 563.2877; found, 563.2889.

3-(4-(4-amino-1H-pyrazolo[3,4-d]pyrimidin-3-yl)phenoxy)-N-(3-fluoro-4-((4-methylpiperazin-1- yl)methyl)phenyl)-4-methylbenzamide ***(6o)***. Prepared in the same manner as **6a**. Yield: 39.5%, mp: 148~150 °C. ^{1}H NMR (300 MHz, DMSO-d_6) δ 13.60 (s, 1H), 10.34 (s, 1H), 8.24 (s, 1H), 7.80–7.67 (m, 4H), 7.63–7.53 (m, 3H), 7.36 (d, J = 8.8 Hz, 1H), 7.12 (d, J = 8.6 Hz, 2H), 3.59 (s, 2H), 2.42 (s, 4H), 2.36 (s, 4H), 2.23 (s, 3H), 2.17 (s, 3H). HRMS (ESI+) m/z calculated for $\mathbf{C_{31}H_{31}FN_8O_2}$ [M+H]$^+$, 567.2627; found, 567.2630.

3-(4-(4-amino-1H-pyrazolo[3,4-d]pyrimidin-3-yl)phenoxy)-N-(3-fluoro-4-(morpholinomethyl)-phenyl)-4-methylbenzamide ***(6p)***. Prepared in the same manner as **6a**. Yield: 44.0%, mp: 188~189 °C. ^{1}H NMR (300 MHz, DMSO-d_6) δ 13.56 (s, 1H), 10.31 (s, 1H), 8.21 (s, 1H), 7.78–7.70 (m, 2H), 7.70–7.63 (m, 2H), 7.61–7.50 (m, 3H), 7.33 (d, J = 8.7 Hz, 1H), 7.09 (d, J = 8.5 Hz, 2H), 3.56 (d, J = 5.5 Hz, 6H), 2.39 (t, J = 4.6 Hz, 4H), 2.20 (s, 3H). HRMS (ESI+) m/z calculated for $\mathbf{C_{30}H_{28}FN_7O_3}$ [M+H]$^+$, 554.2310; found, 554.2318.

3-(4-(4-amino-1H-pyrazolo[3,4-d]pyrimidin-3-yl)phenoxy)-N-(3-chloro-4-((4-methylpiperazin-1-yl)methyl)phenyl)-4-methylbenzamide ***(6q)***. Prepared in the same manner as **6a**. Yeld: 44.0%, mp: 164~166 °C. ^{1}H NMR (300 MHz, DMSO-d_6) δ 13.56 (s, 1H), 10.34 (s, 1H), 8.21 (s, 1H), 7.98 (s, 1H), 7.86 (d, J = 8.0 Hz, 1H), 7.66 (d, J = 8.2 Hz, 2H), 7.63–7.54 (m, 3H), 7.33 (d, J = 8.2 Hz, 1H), 7.09 (d, J = 8.2 Hz, 2H), 3.60 (s, 2H), 2.44 (s, 4H), 2.33 (s, 4H), 2.20 (s, 3H), 2.16 (s, 3H). HRMS (ESI+) m/z calculated for $\mathbf{C_{31}H_{31}ClN_8O_2}$ [M+H]$^+$, 583.2331; found, 583.2340.

3-(4-(4-amino-1H-pyrazolo[3,4-d]pyrimidin-3-yl)phenoxy)-N-(3-chloro-4-(morpholinomethyl)- phenyl)-4-methylbenzamide ***(6r)***. Prepared in the same manner as **6a**. Yield: 61.0%, mp: 198~200 °C. ^{1}H NMR (300 MHz, DMSO-d_6) δ 13.58 (s, 1H), 10.37 (s, 1H), 8.24 (s, 1H), 8.02 (d, J = 1.7 Hz, 1H), 7.90 (dd, J = 8.0, 1.8 Hz, 1H), 7.73–7.57 (m, 5H), 7.36 (d, J = 8.3 Hz, 1H), 7.15–7.08 (m, 2H), 3.62 (dd, J = 8.0, 3.6 Hz, 6H), 2.45 (t, J = 4.6 Hz, 4H), 2.23 (s, 3H). ^{13}C NMR (75 MHz, DMSO-d_6) δ 164.34, 158.54, 158.03, 156.52, 156.24, 153.89, 144.41, 139.37, 138.81, 135.47, 133.76, 131.87, 131.17, 130.49, 128.74, 128.32, 126.84, 125.01, 118.05, 116.81, 112.26, 97.38, 66.65, 59.24, 53.70, 15.88. IR (cm^{-1}): 3461.27, 3411.61, 3300.06, 3091.84, 2965.77, 2853.38, 2814.50, 1670.93, 1644.14, 1601.02, 1586.29, 1534.44, 1507.30,

1459.30, 1449.19, 1436.63, 1411.32, 1313.30, 1290.46, 1264.71, 1233.95, 1218.70, 1168.25, 1158.02, 1110.25, 1006.58, 990.06, 909.18, 864.18, 848.53, 814.36, 801.96,740.84. HRMS (ESI+) *m/z* calculated for $\mathbf{C_{30}H_{28}ClN_7O_3}$ $[M+H]^+$, 570.2015; found, 570.2022.

3-(4-(4-amino-1H-pyrazolo[3,4-d]pyrimidin-3-yl)phenoxy)-N-(3-bromo-4-((4-methylpiperazin-1-yl)methyl)phenyl)-4-methylbenzamide ***(6s)***. Prepared in the same manner as **6a**. Yield: 44.0%, mp: 180~181 °C. ^{1}H NMR (300 MHz, DMSO-d_6) δ 13.59 (s, 1H), 10.38 (s, 1H), 8.24 (s, 1H), 8.17 (s, 1H), 7.93 (d, J = 8.1 Hz, 1H), 7.69 (d, J = 8.2 Hz, 2H), 7.65–7.56 (m, 3H), 7.36 (d, J = 8.0 Hz, 1H), 7.11 (d, J = 8.2 Hz, 2H), 3.61 (s, 2H), 2.43 (s, 8H), 2.23 (s, 6H). HRMS (ESI+) *m/z* calculated for $\mathbf{C_{31}H_{31}BrN_8O_2}$ $[M+H]^+$, 627.1826; found, 627.1823.

3-(4-(4-amino-1H-pyrazolo[3,4-d]pyrimidin-3-yl)phenoxy)-N-(3-bromo-4-(morpholinomethyl)- phenyl)-4-methylbenzamide ***(6t)***. Prepared in the same manner as **6a**. Yield: 27.7%, mp: 189~190 °C. ^{1}H NMR (300 MHz, DMSO-d_6) δ 13.59 (s, 1H), 10.38 (s, 1H), 8.24 (s, 1H), 8.19 (d, J = 1.7 Hz, 1H), 7.94 (dd, J = 8.0, 1.8 Hz, 1H), 7.75–7.56 (m, 5H), 7.36 (d, J = 8.1 Hz, 1H), 7.16–7.07 (m, 2H), 3.63 (d, J = 5.5 Hz, 6H), 2.46 (t, J = 4.6 Hz, 4H), 2.23 (s, 3H). HRMS (ESI+) *m/z* calculated for $\mathbf{C_{30}H_{28}BrN_7O_3}$ $[M+H]^+$, 614.1510; found, 614.1513.

N-(3-(4-(4-amino-1H-pyrazolo[3,4-d]pyrimidin-3-yl)phenoxy)phenyl)-4-((4-methylpiperazin-1- yl)methyl)-3-(trifluoromethyl)benzamide ***(6u)***. Prepared in the same manner as **6a**. Yield: 38.7%, mp: 146~148 °C. ^{1}H NMR (300 MHz, DMSO-d_6) δ 13.55 (s, 1H), 10.51 (s, 1H), 8.23 (s, 3H), 7.92 (d, J = 8.0 Hz, 1H), 7.74–7.66 (m, 2H), 7.61 (dd, J = 8.5, 1.2 Hz, 2H), 7.42 (t, J = 8.3 Hz, 1H), 7.26–7.17 (m, 2H), 6.95–6.86 (m, 1H), 6.75 (s, 1H), 3.68 (s, 2H), 2.43 (s, 4H), 2.37 (s, 4H), 2.18 (s, 3H). HRMS (ESI+) *m/z* calculated for $\mathbf{C_{31}H_{29}F_3N_8O_2}$ $[M+H]^+$, 603.2438; found, 603.2442.

4.3. In vitro kinase assay

The effects of compounds on the kinases DDR1 were assessed using a LanthaScreen Eu kinase activity assay technology (Invitrogen). Kinase reactions are performed in a 10 μL volume in low-volume 384-well plates. The kinases in the reaction buffer consist of 50 mM HEPES pH 7.5, 0.01% Brij-35, 10 mM $MgCl_2$, and 1 mM EGTA; the concentration of the fluorescein-poly GAT substrate (Invitrogen) in the assay is 100 nM. Kinase reactions were initiated with the addition of 100 nM ATP in the presence of serials of dilutions of compounds. The reactions were allowed to proceed for 1 h at room temperature before a 10 μL preparation of EDTA (20 mM) and Eu-labeled antibody (4 nM) in time-resolved TR-FRET dilution buffer are added. The final concentration of antibody in the assay well is 2 nM, and the final concentration of EDTA is 10 mM. The plate is allowed to incubate at room temperature for one more hour before the TR-FRET emission ratios of 665/340 nm were acquired on a PerkinElmer EnVision multilabel reader (Perkin-Elmer, Inc.). Data analysis and curve fitting were performed using GraphPad Prism 7 software.

4.4. Inhibition on cell proliferation by MTT assay

Adherent cells were plated in 96-well culture plates with cell density of 3000–4000 cells/well and treated with indicated compounds by adding 100 μL of medium containing compounds of various concentrations on the second day. After 72 h of treatment, MTT was added to each well and incubated for additional 4–5 h, and the absorbance was measured on a microplate reader at 570 nm. Cell growth inhibition was evaluated as the ratio of the absorbance of the sample to that of the control.

4.5. Molecular docking assay

Molecular docking of the compound **6c** into the three dimensional X-ray structure of DDR1 was carried out using the Discovery Studio (Version 4.0) as implemented through the graphical user interface Discovery Studio CDOCKER protocol. The crystal structure of DDR1 (PDB ID: 4CKR) was obtained from the Protein Data Bank. All bound waters and ligands were eliminated from the protein and the polar hydrogens were added. The whole 4CKR was defined as a receptor and the binding site was selected based on ATP binding site of 4CKR. The three-dimensional structure of the compound **6c** was constructed using ChemBio 3D Ultra 14.0 software and **6c** was given CHARMm forcefield. The compound **6c** was placed during the molecular docking procedure. Types of interactions of the docked protein with ligand were analyzed after the end of molecular docking.

Declaration of Competing Interest

The authors declare that they have no known competing financial interests or personal relationships that could have appeared to influence the work reported in this paper.

Acknowledgments

This work was supported by the College Students Innovation Training program. We thank Prof. Xiaoyun Lu for helps in DDR1 kinase inhibition assay.

References

1 Fu HL, Sohail A, Valiathan RR, et al. Shedding of discoidin domain receptor 1 by membrane-type matrix metalloproteinases. *J Biol Chem*. 2013;288:12114–12129.
2 Auguste P, Leitinger B, Liard C, Rocher V, Azema L, Saltel F, Santamaria D. Meeting report - first discoidin domain receptors meeting. *J Cell Sci*. 2020;133:jcs243824.
3 Valiathan RR, Marco M, Leitinger B, Kleer CG, Fridman R. Discoidin domain receptor tyrosine kinases: new players in cancer progression. *Cancer Metastasis Rev*. 2012;31:295–321.
4 Avivi-Green C, Singal M, Vogel WF. Discoidin domain receptor 1-deficient mice are resistant to bleomycin-induced lung fibrosis. *Am J Respir Crit Care Med*. 2006;174:420–427.
5 Flamant M, Placier S, Rodenas A, et al. Discoidin domain receptor 1 null mice are protected against hypertension-induced renal disease. *J Am Soc Nephrol*. 2006;17:3374–3381.
6 Gross O, Girgert R, Beirowski B, et al. Loss of collagen-receptor DDR1 delays renal fibrosis in hereditary type IV collagen disease. *Matrix Biol*. 2010;29:346–356.
7 Franco C, Hou G, Ahmad PJ, et al. Discoidin domain receptor 1 (DDR1) deletion decreases atherosclerosis by accelerating matrix accumulation and reducing inflammation in low-density lipoprotein receptor-deficient mice. *Circ Res*. 2008;102:1202–1211.
8 Ahmad PJ, Trcka D, Xue S, et al. Discoidin domain receptor-1 deficiency attenuates atherosclerotic calcification and smooth muscle cell-mediated mineralization. *Am J Pathol*. 2009;175:2686–2696.
9 Franco C, Britto K, Wong E, et al. Discoidin domain receptor 1 on bone marrow-derived cells promotes macrophage accumulation during atherogenesis. *Circ Res*. 2009;105:1141–1148.
10 Jeitany M, Leroy C, Tosti P, et al. Inhibition of DDR1-BCR signalling by nilotinib as a new therapeutic strategy for metastatic colorectal cancer. *EMBO Mol Med*. 2018;10:e7918.
11 Vehlow A, Cordes N. DDR1 (discoidin domain receptor tyrosine kinase 1) drives glioblastoma therapy resistance by modulating autophagy. *Autophagy*. 2019;15:1487–1488.
12 Vehlow A, Klapproth E, Jin S, et al. Interaction of discoidin domain receptor 1 with a 14-3-3-Beclin-1-Akt1 complex modulates glioblastoma therapy sensitivity. *Cell Rep*. 2019;26:3672–3683.
13 Duncan JS, Whittle MC, Nakamura K, et al. Dynamic reprogramming of the kinome in response to targeted MEK inhibition in triple-negative breast cancer. *Cell*. 2012;149:307–321.
14 Das S, Ongusaha PP, Yang YS, Park JM, Aaronson SA, Lee SW. Discoidin domain receptor 1 receptor tyrosine kinase induces cyclooxygenase-2 and promotes chemoresistance through nuclear factor-κB pathway activation. *Cancer Res*. 2006;66:8123–8130.
15 Miao L, Zhu S, Wang Y, et al. Discoidin domain receptor 1 is associated with poor prognosis of non-small cell lung cancer and promotes cell invasion via epithelial-to-mesenchymal transition. *Med Oncol*. 2013;30:626.
16 Gao M, Duan L, Luo J, et al. Discovery and optimization of 3-(2-(Pyrazolo[1,5-a]pyrimidin-6-yl)ethynyl)benzamides as novel selective and orally bioavailable discoidin domain receptor 1 (DDR1) inhibitors. *J Med Chem*. 2013;56:3281–3295.
17 Kim HG, Tan L, Weisberg EL, et al. Discovery of a potent and selective DDR1 receptor tyrosine kinase inhibitor. *ACS Chem Biol*. 2013;8:2145–2150.
18 Wang Z, Bian H, Bartual SG, et al. Structure-based design of tetrahydro- isoquinoline-7-carboxamides as selective discoidin domain receptor 1 (DDR1) inhibitors. *J Med Chem*. 2016;59:5911–5916.

19 Wang Z, Zhang Y, Bartual SG, et al. Tetrahydroisoquinoline-7-carboxamide derivatives as new selective discoidin domain receptor 1 (DDR1) inhibitors. *ACS Med Chem Lett*. 2017;8:327–332.
20 Vanajothi R, Hemamalini V, Jeyakanthan J, Premkumar K. Ligand-based pharmacophore mapping and virtual screening for identification of potential discoidin domain receptor 1 inhibitors. *J Biomol Struct Dyn*. 2019;38:2800–2808.
21 Zhu D, Huang H, Pinkas DM, et al. 2-Amino-2,3-dihydro-1*H*-indene-5-carboxamide-based discoidin domain receptor 1 (DDR1) inhibitors: design, synthesis, and in vivo antipancreatic cancer efficacy. *J Med Chem*. 2019;62:7431–7444.
22 Wei Z-W, Zhang C-H, He Y. 7rh, a novel selective discoidin domain receptor 1 (DDR1) inhibitor, enhances 5-fluorouracil response in gastric cancer. *Ann Oncol*. 2017;28:iii18.
23 Ma DW, Cai Q. N, N-Dimethyl glycine-promoted Ullmann coupling reaction of phenols and aryl halides. *Org Lett*. 2003;5:3799–3802.
24 Li X, Wang A, Yu K, et al. Discovery of (R)-1-(3-(4-amino-3-(4-phenoxyphenyl)-1*H*-pyrazolo[3,4-*d*]pyrimidin-1-yl)piperidin-1-yl)-2-(dimethyl-amino)ethanone (CHMFL-FLT3-122) as a potent and orally available FLT3 kinase inhibitor for FLT3-ITD positive acute myeloid leukemia. *J Med Chem*. 2015;58:9625–9638.
25 Su J, Ding K, Zhao H, et al. Anti-pulmonary fibrosis application of DDR2 small-molecule inhibitor. *CN104490889 (A)*. 2015.